JOURNAL OF MATERIALS SCIENCE: MATERIALS IN MEDICINE **16** (2005) 909–917

Microstructural and *in vitro* characterization of SiO_2-Na_2O-CaO-MgO glass-ceramic bioactive scaffolds for bone substitutes

C. VITALE–BROVARONE[1,*], E. VERNÈ[1], M. BOSETTI[2], P. APPENDINO[1], M. CANNAS[2]
[1]*Materials Science and Chemical Engineering Department, Polytechnic of Torino, C.so Duca degli Abruzzi 24, 10129 Torino, Italy*
[2]*Department of Medical Sciences, Human Anatomy, University of Eastern Piedmont, Novara, Italy*
E-mail: chiara.vitale@polito.it

In the present research work, the preparation and characterization of bioactive glass-ceramic scaffolds for bone substitutes are described. The scaffolds were prepared by starch consolidation of bioactive glass powders belonging to the SiO_2-Na_2O-CaO-MgO system using three different organic starches (corn, potatoes and rice) as reported in a previous screening process [1]. The scaffolds, characterized by scanning electron microscopy, showed a porous structure with highly interconnected pores. The pores sizes assessed by mercury intrusion porosimetry put in evidence the presence of pores of 50–100 μm. The structure of the scaffolds was investigated by X-ray diffraction and revealed the glass-ceramic nature of the obtained material. The mechanical properties of the scaffolds were evaluated by means of compressive tests on cubic samples and the obtained results demonstrated their good mechanical strength. The *in vitro* bioactivity of the scaffolds was tested by soaking them in a simulated body fluid (SBF) and by subsequently characterizing the soaked surfaces by SEM, EDS and X-ray diffraction. Good *in vitro* bioactivity was found for the starting glass and for the obtained scaffolds. Moreover, the scaffold bioresorption, tested by measuring the samples weight loss in SBF at different periods of time, showed a partial resorption of the scaffolds. Cell culture testing of the three different scaffolds indicated no differences in cell number and in alkaline phosphatase activity; the morphology of the osteoblasts showed good spreading, comparable to bulk material which was used as the control.

1. Introduction

In the last few years, the need for suitable materials to filling bone defects had interested many research groups. In fact, the demand for bone grafts is high and their uses are multiple due to bone loss or tumors, periodontal resorption and arthroplasty revision surgery [2–4]. At present, autologous bone still represents the gold standard for a bone graft, but its limited availability and the risk of donor site morbidity stresses the need for finding alternative solutions [5–6]. On the other hand, the use of allogenic/xenogenic implants involves a significant risk of viral transmission and generally has a bioresorption rate which is not suitable with the bone healing process [7–9]. On the contrary, alloplastic biomaterials, being synthetic, completely overcome antigenicity problems, morbidity and are available in unlimited amounts. As far as synthetic materials for bone grafts are concerned, a few ceramics are of great interest due to the lack of cytotoxicity and to their osteoconductive properties. These include hydroxyapatite and tricalcium phosphate which have been widely investigated [10–14]. Bioactive glasses and glass-ceramics of specific composition represent a very attractive alternative. These glasses, when in contact with physiological media, stimulate the precipitation of an hydroxyapatite layer (HAp) on their surfaces, that in turn promotes effective osteointegration of the implant [15–18]. Aiming to simulate the cancellous bone structure and to improve their osteointegration, these biomaterials can be produced in a porous form as a scaffold. If sufficient pores sizes (i.e. greater than 50–100 μm) with a highly interconnected structure are obtained, a fast vascularisation of the implant and the promotion of the bone in-growth process can be expected.

Up to now, many methods have been proposed to obtain porous materials [2–4, 10, 19–24] and amongst

*Author to whom all correspondence should be addressed.

them, the consolidation of a ceramic suspension is one of the more reliable, low-cost ones which allows the formation of complex shapes. With this aim, starch powders are used as consolidation agents of a glass powder suspension, due to their ability of absorbing great amount of water if heated above their gelatinization temperature (70 °–80 °C) [25–27]. If an optimum starch/water ratio is used, during the starch gelation, the amount of available water steadily decreases and eventually, the ceramic powders come in intimate contact and stick together. Besides, the swelled starches are absorbed on the ceramic powder surface and, due to their binding effect, they impart a sufficient mechanical strength to the consolidated body which can be easily de-moulded and handled. Once the ceramic-starch material is consolidated, the swelled starch powders are thermally removed, acting as pore formers. A sintering treatment is then carried out on the resultant porous body, in order to impart sufficient mechanical strength. In fact, the inherent mechanical weakness of a macroporous ceramic scaffold is of concern but on the other hand, a highly porous structure is needed to allow proper bone in growth and vascularization of the implant. Aiming to maximize the mechanical strength of the scaffold and to reduce as much as possible the risk of undesired failure, a flawless material with dense strut walls is required. After implantation of the scaffold, its mechanical strength increases with time as the bone in-growth process completeness reaches. Due to these factors, it is clear that a bioactive material which promotes the bone regeneration process is highly desirable. Moreover the crystallization of a specific phase with peculiar mechanical or biological properties can be obtained with a fine tuning of the glass composition and of the sintering treatment. The glass composition can also be tailored to obtain a material with a significant degree of bioresorption which in vivo would be gradually replaced by healthy, new grown bone tissue.

For these considerations, the starch consolidation of bioactive glass powders was chosen, and the glass composition was set considering previous studies [1, 28, 29].

In our research, the main factors affecting the final porous structure and its properties are: total solid loading, amount and particle size of the starch powders, consolidation and burning-out treatments, sintering conditions and glass powders size. These parameters were set on the basis of previous investigations reported elsewhere [1], and a complete characterization of the obtained material was carried out.

2. Materials and methods

In order to obtain a porous structure, organic and inorganic materials were used in this study. The chosen organic phase consisted of three commercial, low-cost starch powders that were used as a consolidation agent and as pore formers.

For this aim a suspension containing both starch and glass powders was used and after the consolidation occurred, the swelled starch powders were thermally removed for obtaining a porous material. After the removal of the organic part, the porous body was sintered to impart mechanical strengths.

The glass composition was chosen on the basis of previous works [1, 28, 29] in order to obtain a highly bioactive material containing a significant amount of magnesium that it is known to positively affect many cellular functions [30, 31]. The chosen glass(SNCM) belongs to the system SiO_2-Na_2O-CaO-MgO and has the following composition: SiO_2 (50% mol), Na_2O (25% mol), CaO (16% mol), MgO (9% mol). SNCM was prepared by melting the starting products at 1500 °C in a platinum crucible and by quenching the melt in cold water. The resultant frit was ball milled for obtaining powders that were sieved below 100 μm. SNCM bars were produced by pouring the melt on a preheated stainless steel plate for evaluating the *in vitro* bioactivity of the starting glass. Some SNCM bars underwent a thermal treatment analogous to the proposed sintering one so that a glass-ceramic structure was obtained (GC-SNCM). The scaffolds preparation route involved several steps. Starch and SNCM powders were mixed with a proper amount of distilled water, obtaining a suspension. The suspension was stirred for 1h while increasing the temperature to 70 °–80 °C at which, the prompt water uptake of the starches occurred, leading to a gel-like material. The gel was poured in a metallic mould and underwent a consolidation treatment; the consolidated material was then de-moulded and underwent a thermal treatment leading to the burning-out of the organic phase and the sintering of the inorganic one.

On the basis of a previous work [1], in which it was observed that for the chosen set of starch and SNCM powders, the starch range between 20 and 26 wt% was the most promising one, it was decided to set it at 23 wt%.

All the processing parameters were chosen on the basis of this previous optimization step and set as follows:

– Starch content: 23 wt%
– Starch powders sieved above 60 μm; Glass powders sieved below 100 μm;
– Total solid loading: 40 wt% (it allows to attain an even shrinkage of the consolidated body and a complete swelling of the starch powders);
– Consolidation treatment: 30 min at 40 °–50 ° and 60 °C, 2 h at 70 °C and 10 h at 80 °C;
– Burning out and sintering phase in a single step: slow heating to 300 °C, maintenance for 1 h, slow heating to 900 °C (1 °C/min) with maintenance for 3 h aiming to sinter the scaffold. The burning-out phase and the sintering treatment were unified aiming to simplify the preparation procedure and to avoid crack formation during the manipulation of the unsintered green body.

Three different organic starches were used to prepare the scaffolds and the obtained porous materials will be named from now on as C23, P23 and R23 on the basis of the used type starch (Corn, Potatoes and Rice respectively) and its wt% amount.

2.1. Scaffold characterisation

The quality of the scaffolds was assessed by SEM observations (SEM Philips 525 M) aiming to verify the absence of cracks and the degree of densification of the sintering necks between SNCM particles.

A series of SEM evaluations was carried out to observe the morphology of the pores, the degree of their interconnectivity and the homogeneity of their distribution along the sections of the scaffolds. In such a way, the differences between C23, P23 and R23 samples were evaluated.

Moreover, the volume of the pores and their size distribution were assessed by mercury intrusion porosimetry (Porosimeter 2000 Fisons).

The proposed sintering treatment involved extensive crystallization taking place in the chosen glass and the nature of the crystallized phases was investigated by means of X-ray analysis (X'Pert Philips diffractometer) using the Bragg Brentano camera geometry and Cu K_α incident radiation.

The compressive strength of the sintered scaffolds was evaluated using Schenck-Trabel equipment on cubic specimens ($10 \times 10 \times 10$ mm size) obtained by cutting the prepared scaffolds with a diamond blade. The test was carried out following ASTM C773-88 Standard Test Method, with a slight modification due to the use of cubic samples instead of cylindrical ones.

The amount of scaffold resorption was evaluated using weight loss measurements on cubic samples which were soaked in a simulated body fluid with the same inorganic composition of human plasma (SBF) [32] for times varying between 2 weeks up to 3 months. As well as weight loss measurements, the ions which leached into the solution and the effect of resorption on the microstructure of the scaffolds were observed using SEM and EDS analyses after soaking in SBF.

2.2. Soaking in simulated body fluid

The prepared SNCM and GC-SNCM bars were tested *in vitro* for comparing the bioactivity of glass and glass-ceramic SNCM.

The *in vitro* bioactivity of both the bars and the prepared scaffolds was investigated by soaking them in SBF. When a bioactive glass is in contact with physiological media the formation of a silica gel layer occurs on its surface due to ions leaching and condensation of silanols, afterwards, on top of it, calcium phosphates precipitate and crystallize forming a hydroxyapatite layer (HAp). The HAp precipitation occurs after period of soaking varying from days to a few weeks. On our samples, the precipitation of the HAp layer was evaluated by means of SEM and EDS analyses. The formation of the silica gel and the crystallization of the Ca-P rich layer precipitated on the soaked surfaces was studied using X-ray diffraction.

2.3. Cell behavior

Cell behavior on the materials tested was studied using osteoblasts-like cells obtained by enzymatic isolation from trabecular fragments of adult human bone removed during surgery and treated as described in the literature [33]. A cell density of 2×10^4 cells/cm^{2}has been used for every observation.

Since the tested materials were not suitable for normal light microscopy, we observed cell morphology and distribution with fluorescence microscopy and scanning electron microscopy (SEM). After 4 days of osteoblast-like cell proliferation, the materials tested were rinsed in phosphate buffer solution (PBS), fixed for 20 min at 60 °C and stained for 5 min in a 0,025% Acridine Orange solution which is a nucleic acid staining [34]. The cell morphology and number on each material were evaluated using an Aristoplan fluorescent microscope (Leitz Leica, Milano, Italy). The osteoblast-like cell number was evaluated on a surface of 0.0682 mm^2 using a 40X microscope magnification and the mean ± standard deviation of 30 fields was obtained from 3 different experiments.

SEM analysis was performed on cells cultured for 4 days on the incubated materials. After washing with cacodylate buffer (pH 7.4), cells were fixed in Karnowsky's solution (4% paraformaldehyde + 2.5% glutaraldehyde in 0.1 M cacodylate buffer pH 7.4) for 30 min at 4 °C. After washing in cacodylate buffer, cells were dehydrated in ethanol (50–100%) and then in hexamethyldisilazane [35]. The materials were then mounted onto appropriate stubs and observed under an SEM (Philips 525 M).

Alkaline phosphatase activity (APA), a marker of osteoblast-like cell differentiation, was determined by an assay based on the hydrolysis of p-nitrophenylphosphate to p-nitrophenol. Cultures were collected after 4 days incubation on the materials, rinsed three times with PBS and then placed into 300 μl of 0.05% Triton X100 in PBS and sonicated on ice for 2×10 sec using a Branson 250 sonifier (Branson Ultrasonics, Danbury, USA). One hundred microliters of solution (1 mM p-nitrophenilphosphate in 1 M diethanolamine +1 mM $MgCl_2$ pH 9.8 all from Sigma) was added to 100 μl of cell extract. The mixture was incubated at 37 °C for 15–30 min until the colour was comparable with a standardised series (a 20 mM p-nitrophenol solution from Sigma). All samples, including the standardised series (1 μM-7 nM), were measured in duplicate on a Bio-Rad microplate spectrophotometer at 410 nm [36].

3. Results and discussion

Fig. 1(a) and (b) show two micrographs of SNCM surfaces after soaking in SBF for different periods of time. After 2 weeks in SBF (Fig. 1(a)), the glass surface is uniformly covered by a silica gel and on top of it few HAp globular agglomerates can be seen. For longer soaking periods, an increase in the amount in precipitated HAp on top of the silica gel was observed. The EDS results reported in Fig. 1(c) revealed the presence of Ca, P and Si which can be ascribed to HAp agglomerates and to the silica gel underneath them.

The modifications induced by soaking SNCM in SBF were also investigated by X-ray diffraction. Fig. 2 compares the diffraction patterns of as prepared SNCM and

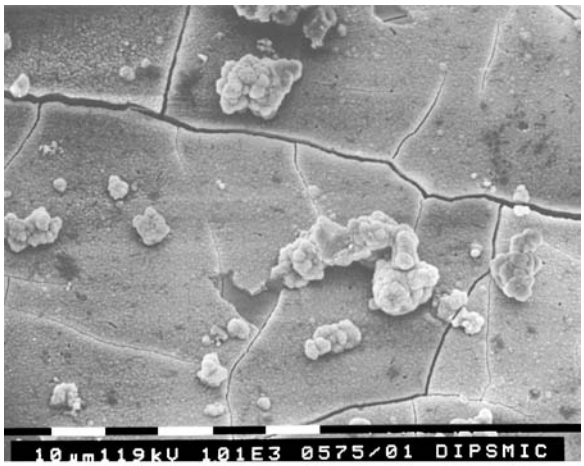

(a)

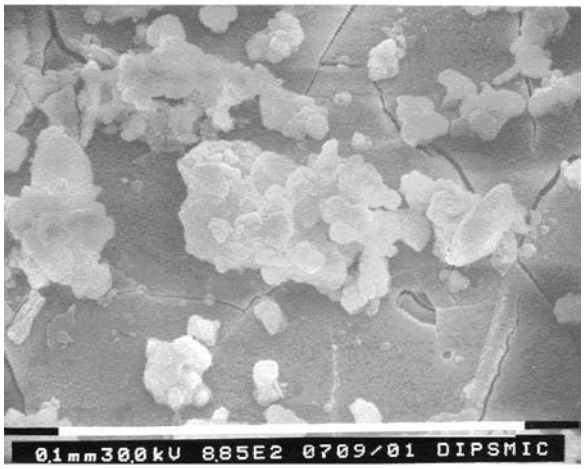

(b)

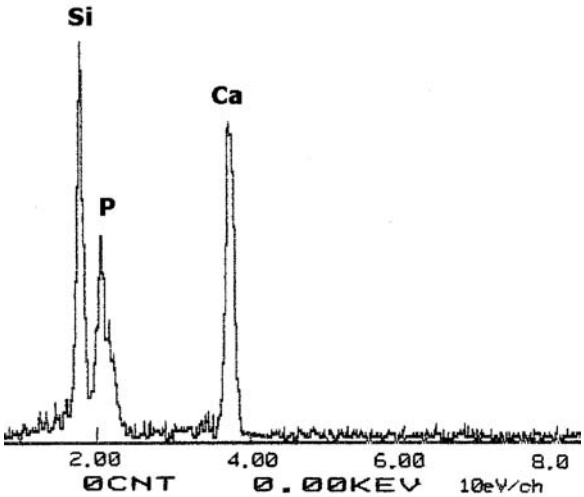

(c)

Figure 1 Micrographs of as done SNCM after 2 weeks (a) and 4 weeks (b) of soaking in SBF; EDS analysis on the whole area reported in Fig. (b) and (c).

of SNCM after 2 and 4 weeks in SBF, respectively. The as-prepared SNCM pattern shows only an amorphous halo and thus indicates that the starting material was amorphous. After 2 weeks in SBF the diffraction pattern revealed the presence of an amorphous halo and a broad signal at 31 °–32 ° degrees two theta. The amorphous halo was detected at a lower diffraction angle than for the as-prepared SNCM due to the formation of

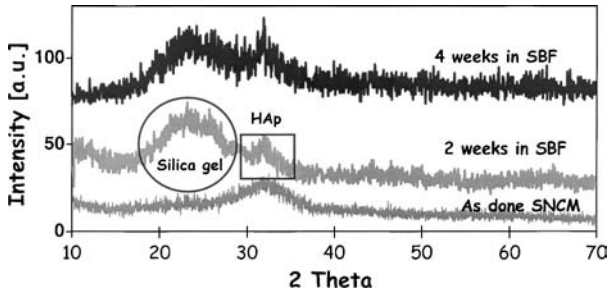

Figure 2 X-ray diffraction patterns of as done SNCM before and after soaking in SBF for 2 and 4 weeks.

the silica gel layer, whereas the broad peaks in the rectangle were identified as HAp. After 4 weeks in SBF, an increase in the amount of HAp was observed because the intensity of the diffraction peaks became more intense. However, the silica gel halo was still visible after 4 weeks in SBF demonstrating that the HAp layer did not entirely cover the surface.

The XRD findings agree with the morphological and compositional observations reported in Fig. 1. The precipitated HAp retains a typical microcrystalline nature since a broad signal was detected in good accordance with the leaf-like crystals observed in other works [37, 38]. Moreover, the bioactivity of glass SNCM is expected to be higher *in vivo* since the circulation of

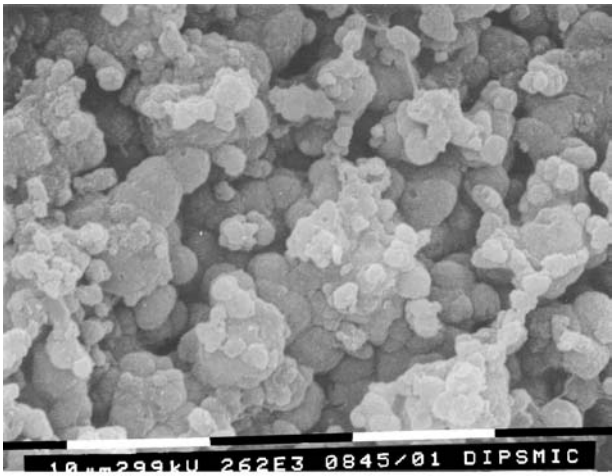

(a)

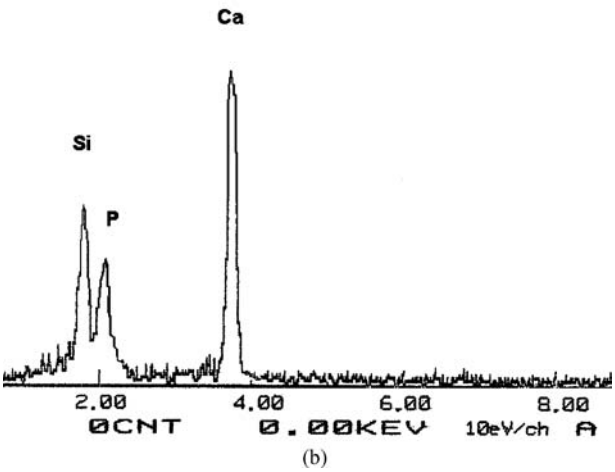

(b)

Figure 3 GC-SNCM after 4 weeks in SBF (a), EDS analysis on the whole area reported in Fig. (a) and (b).

physiological fluid generally involves shorter times for the precipitation of HAp to occur.

The macroporous scaffold preparation involved a thermal treatment above the SNCM crystallization temperature ($T_x = 735$ °C) [1] and thus a glass-ceramic structure was obtained. For the chosen glass composition, the sintering treatment involved the nucleation and growth of $Na_2Ca_2(SiO_3)_3$ crystals and thus all the Mg^{2+} ions are contained in the residual amorphous phase. Aiming to ascertain the effect of the crystallization on the *in vitro* SNCM bioactivity, specimens of bulk SNCM underwent a thermal treatment analogous to the proposed one (GC-SNCM) and were then soaked in SBF. Fig. 3(a) and (b) respectively show a micrograph of GC-SNCM after 4 weeks in SBF and

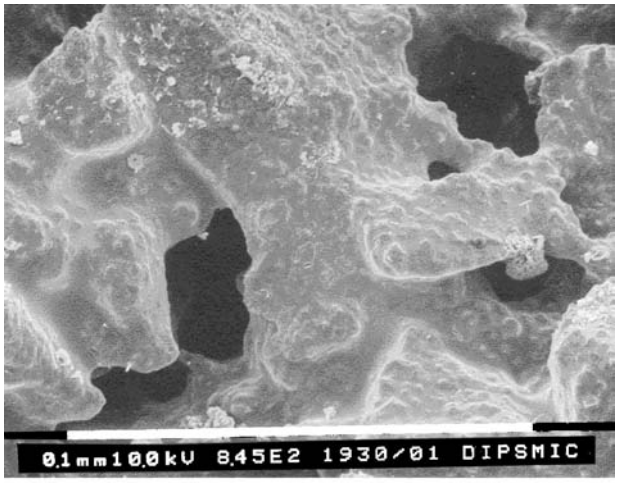

(a)

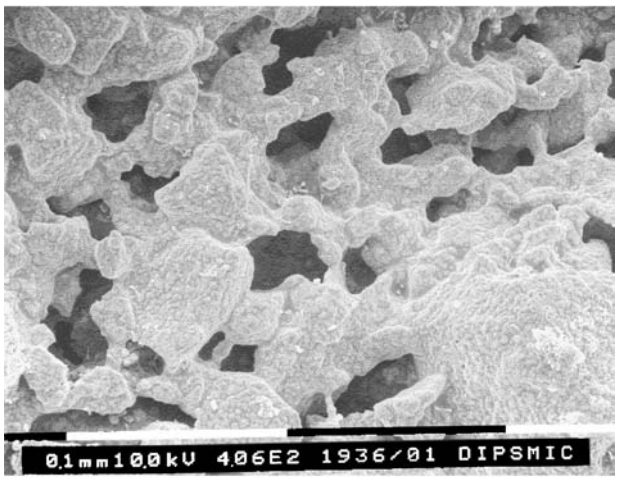

(b)

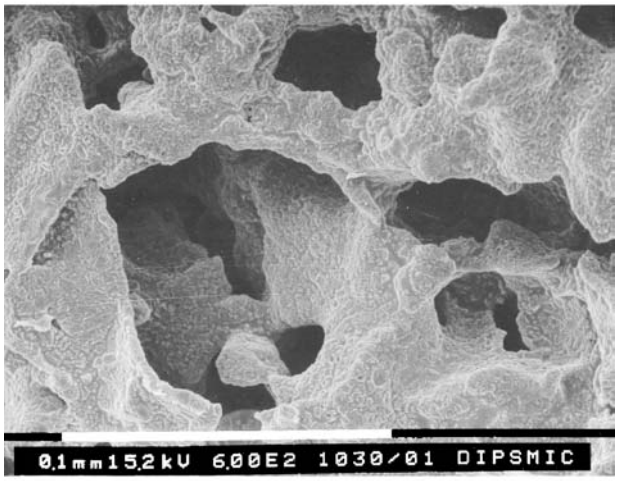

(c)

Figure 4 Micrographs of different scaffolds: C23 (a), P23 (b) and R23 (c) respectively.

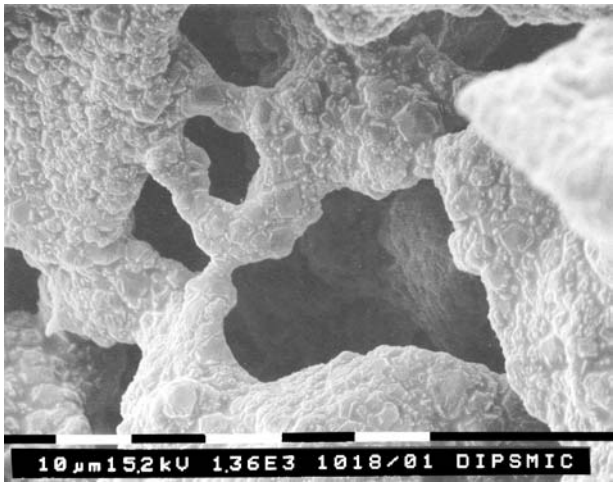

Figure 5 Micrograph of some R23 sintering necks.

(a)

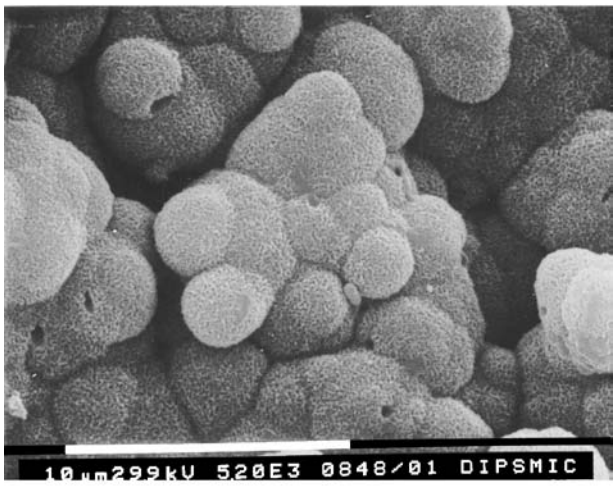

(b)

Figure 6 (a) and (b) Micrographs of R23 after 4 weeks in SBF at different magnifications.

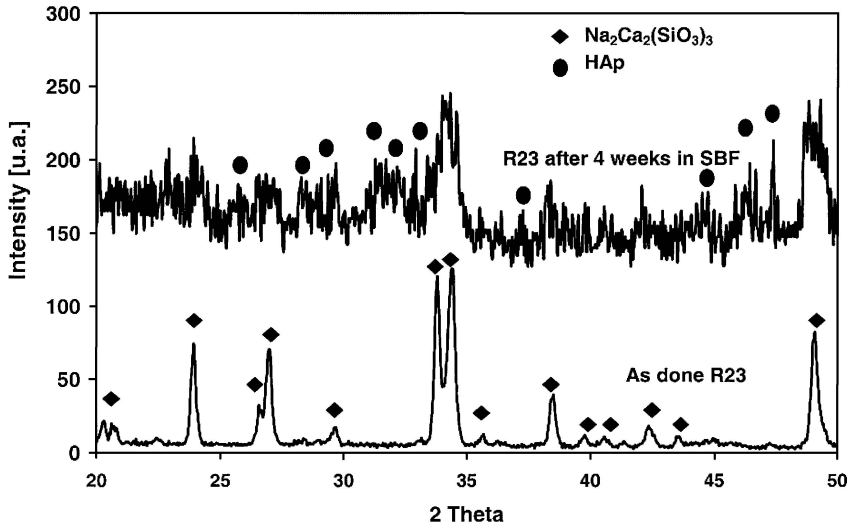

Figure 7 Diffraction patterns of R23 before and after soaking in SBF.

the result of a compositional analysis carried out on the entire soaked surface.

The SBF soaked GC-SNCM was almost completely covered by HAp proving that the presence of $Na_2Ca_2(SiO_3)_3$crystals did not negatively affect the *in vitro* bioactivity of SNCM. When comparing Figs. 1(c) and 3(b), the EDS results seem to confirm the presence of greater amounts of HAp with respect to SNCM. This is not surprising since an equal or even better biological behavior of GC-SNCM was expected as $Na_2Ca_2(SiO_3)_3$is known to have a high bioactivity index [28, 29, 39] .

The procedure previously reported led to the successful preparation of macroporous scaffolds as shown in Fig. 4. Flawless specimens were obtained since no cracks or closed porosities were found.

The pores were homogenously distributed and had an average size varying from 20 to 100 μm depending on the type of starch used. The introduced porosity was highly interconnected and thus satisfied the essential requirement for a properly vascularised implant.

As can be observed in Fig. 4, the R23 scaffolds showed the best results in term of pore size. For this reason some porosimetry studies were carried out on R23 scaffolds in order to achieve a better evaluation of the average pore size and distribution. An average pore size of 84 μm and a pore content of 40% vol. were obtained in good accordance with the morphological findings.

All the scaffolds showed a satisfactory degree of sintering with well densified sintering necks. Fig. 5 shows a micrograph of R23 where a few, well densified sintering necks can be observed.

The glass-ceramic nature of the obtained scaffolds is clearly observable in Figs. 4 and 5 where a non-smooth, uneven surface is shown.

Generally, the mechanical properties of a scaffold can be qualitatively estimated thorugh morphological observations based on the degree of sintering and the presence of microstructural defects. For the proposed scaffolds, satisfactory mechanical properties are expected due to the presence of dense sintering necks, to the homogeneous distribution of the pores and to the absence of defects such as cracks or closed porosities. To support these considerations and to quantify the scaffold maximum strength, compressive tests were carried out on five R23 cubic samples. Compressive strengths of 6

(a)

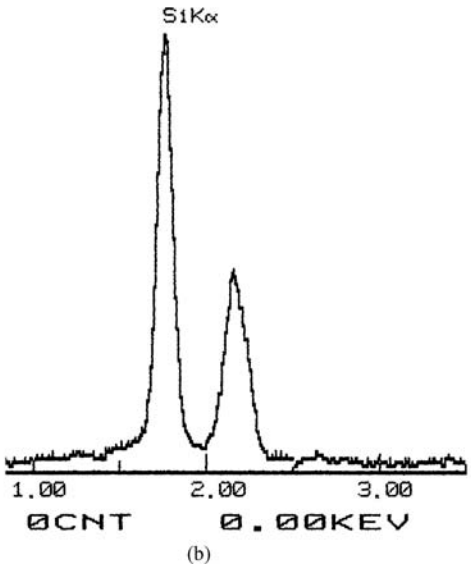

(b)

Figure 8 (a) Micrograph of R23 after SBF (surface non in direct contact with the physiological solution); (b) EDS on the whole area reported in Fig. 8(a).

$\pm$ 1 MPa were found. These values are consistent with the data reported in literature [4, 10, 21, 40, 41]. The obtained standard deviation is not very high and confirms the reproducibility of the proposed method and of the chosen processing parameters.

The bone bonding ability of the scaffolds was investigated by soaking them in SBF. In fact, although the *in vitro* bioactivity of both SNCM and GC-SNCM were assessed, the highly porous microstructure of the scaffolds influences the bioactivity mechanism. Moreover, the scaffolds higher specific surface area will involve a faster ionic exchange with the physiological fluids and a sharper pH increase may be observed. As can be observed in Fig. 6(a), after 4 weeks in SBF, HAp agglomerates are present both inside and outside the pores.

On the basis of these good *in vitro* results, a extensive bone in-growth and vascularisation of the scaffold can be expected. At high magnifications, as can be seen in Fig. 6(b), the globular agglomerates show sub-micronic leaf-like crystals typical of microcrystalline HAp precipitated from solution. The presence of a HAp layer was also assessed by X-ray diffraction as reported in Fig. 7. On R23, before soaking in SBF, only the $Na_2Ca_2(SiO_3)_3$ diffraction peaks were detected whereas a different pattern was found after soaking in SBF.

After 4 weeks in SBF broad signals corresponding to HAp were detected indicating the presence of small crystals according to the leaf-like morphology reported in Fig. 6(b).

Due to the sintering treatment, the obtained scaffolds contained a crystalline phase. For the proposed thermal treatment, the residual amorphous phase is present in small amount as can be deducted by the diffraction pattern of Fig. 6(a) where the amorphous halo of the starting glass almost disappeared. When in contact with physiological fluids, the residual amorphous phase undergoes an ionic exchange and its modifiers ions are leached in the liquid medium. For the scaffolds, due to their porous structure and high specific area, a faster and more extensive ions release than for bulk GC-SNCM was observed. The ions release was remarkable since a significant weight loss could be measured. After 4 weeks in SBF, a weight loss of about 10 wt%. (12 mg/cm^2 of exposed surface) was observed for the three scaffolds showing the partial resorbability of these biomaterials. The microstructural and compositional changes occurring *in vitro* on the scaffolds surface could not be observed in Fig. 6(a). In fact, when

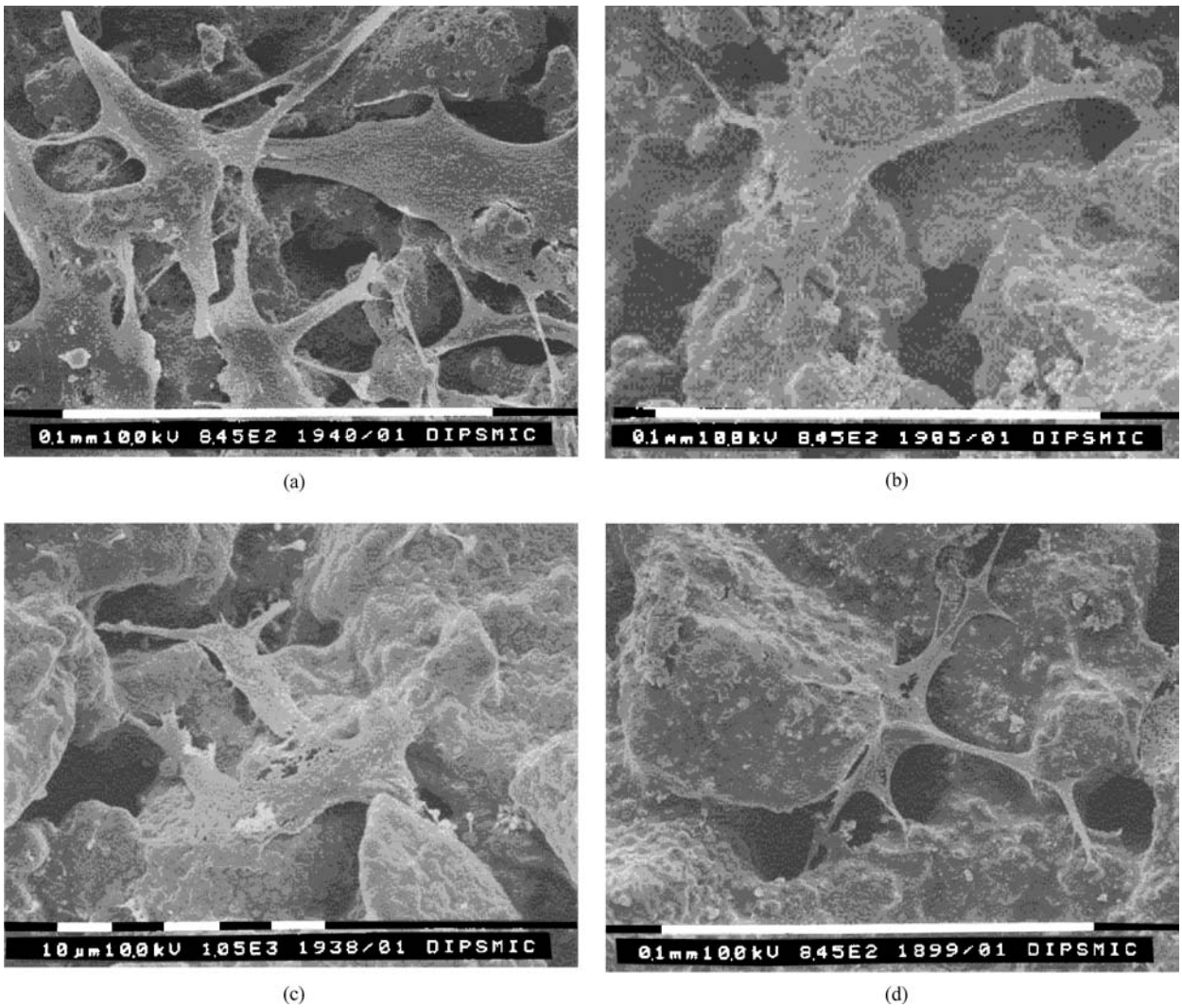

Figure 9 SEM micrographs of osteoblast-like cells cultured on bulk GC-SNCM and on the three scaffolds (C23, P23 and R23).

the scaffold is in contact with physiological fluids, the ions exchange phenomena lead to the precipitation of HAp and thus the scaffold underneath it is difficult to observe. On the contrary, on the lateral surfaces, the precipitation of HAp is more limited and thus the morphology of the partially resorpted scaffold can be observed. For this purpose, Fig. 8(a) shows a lateral view of R23 after 4 weeks in SBF. The EDS analysis carried out on the whole area of Fig. 8(a) is reported in Fig. 8(b) and shows only Si and Au (due to the sample preparation for SEM).

The EDS results showed that probably, after 4 weeks in SBF, all the modifiers ions were almost completely released. When tested *in vivo*, all Mg^{2+} ions would be released in the surrounding fluids and would be available for the surrounding cells. Divalent cations such as Mg^{2+} have been demonstrated to play a critical role in bone remodeling and skeletal development [42, 43]. Recent studies have shown that cation-promoted cell adhesion depends on integrins associated signal transduction pathways and results in enhanced gene expression of extracellular matrix proteins [44] and cellular differentiation [45]. Therefore, Mg^{2+} containing glass-ceramic may be a way to promote optimal osteogenesis and implant integration in skeletal tissue surgery.

Fig. 9 shows a few micrographs related to the osteoblasts proliferations tests carried out on GC-SNCM and on the three prepared scaffolds.

Human osteoblasts cultured on the surfaces of the three materials (C23, P23 and R23) and observed with SEM showed good spreading comparable to bulk material used as control (GC-SNCM). Cells are present on the surfaces of the scaffolds and insides the pores; filopodes frequently seems to make bridges in the porous scaffold. The cell count shown in Fig. 10 and the alkaline phosphatase activity shown in Fig. 11 indicated no great differences between GC-SNCM, C23, P23 and R23, even if a lower cell number resulted from P23.

GC-SNCM and the three scaffolds caused an increase in medium pH. The polystyrene cell culture medium showed a pH 7.58–7.62 while the culture media of cells cultured on the tested materials resulted in a pH between 8.10 and 8.41 with a higher value in the presence of the porous scaffolds due to their higher specific surface area which could be involved in a faster ionic exchange. In particular, we think that Na^+ released in culture media could be exchanged by H^+ ions, increasing pH by H^+

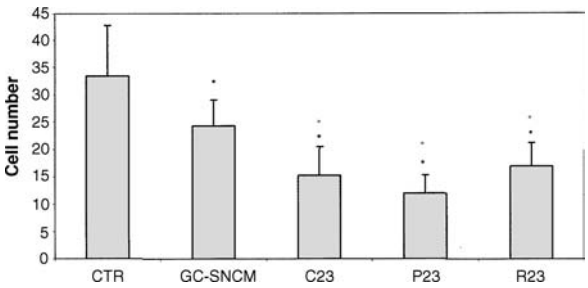

Figure 10 Osteoblast-like cells number at 4 days of proliferation on the tested materials. $^*p < 0.05$ with respect to CTR; $^\circ p < 0.05$ with respect to SNCM.

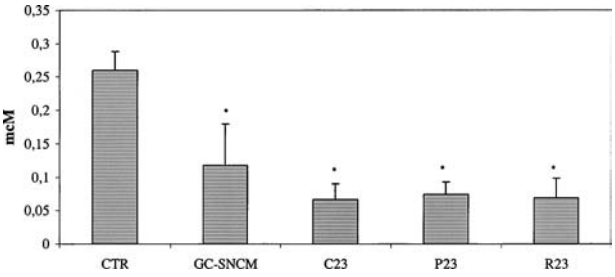

Figure 11 Alkaline phosphatase activity of osteoblast-like cells cultured 4 days on the tested materials. $^*p < 0.05$ with respect to CTR; $^\circ p < 0.05$ with respect to SNCM.

depletion. To evaluate if these pH modifications or Na^+ excess in culture media influenced cell behaviour, we have compared alkaline phosphatase data and cell proliferation results using polystyrene as control. We have showed that cells grown on the three scaffolds and on bulk GC-SNCM resulted statistically lower with lower alkaline phosphatase activity compared to cells grown on polystyrene but no statistical differences were found between the three scaffolds and GC-SNCM. On these bases, we can postulate that during materials incubation in biological fluids, Mg^{2+}, Ca^{2+} but also Na^+ were released in culture medium; while divalent cations influenced positively osteoblast behaviour, Na^+ should be responsible of this negative effect.

4. Conclusions

Using the starch consolidation method and the optimized processing parameters, macroporous scaffolds were successfully prepared. The pores are in the range of 50–100 μm, highly interconnected and in significant amounts. The proposed glass composition and sintering treatment led to a final glass-ceramic structure with a residual amorphous phase enriched with Mg^{2+} ions and $Na_2Ca_2(SiO_3)_3$as the crystalline phase. Due to the composition of the amorphous phase and to thegood bioactivity index of $Na_2Ca_2(SiO_3)_3$, an excellent *in vitro* bioactivity was observed. Moreover the scaffolds showed interesting mechanical properties and a certain degree of resorption.

The three different scaffolds (C23, P23, R23) did not influence human osteoblast-like cell proliferation, alkaline phosphatase activity or cell morphology if compared to bulk material (GC-SNCM) used as control. Aiming to increase the scaffolds biocompatibility, an optimization of the glass composition could be proposed.

References

1. C. VITALE-BROVARONE, S. DI NUNZIO, O. BRETCANU and E. VERNÈ, *J. Mater. Sci. Mater. Med.* **15** (2004) 209.
2. P. SEPULVEDA, J. R. JONES and L. L. HENCH, *J. Biomed. Mater. Res.* **59** (2002) 340.
3. Y. LEE, Y. SEOL, Y. LIM, S. KIM, S. HAN, I. RHYU, S. BAEK, S. HEO, J. CHOI, P. KLOKKEVOLD and C. CHUNG, *ibid.* **54** (2001) 216.
4. P. SEPULVEDA, A. H. BRESSIANI, J. C. BRESSIANI, L. MESEGUER and B. KONIG, *ibid.* **62** (2002) 587.

5. J. C. BANWART, M. A. ASHER and R. S. HASSANEIN, *Spine* **20** (9) (1995) 1055.
6. J. A. GOULET, L. E. SENUNAS, G. L. DESILVA and M. L. GREENFIELD, *Clin. Orthop.* **39** (1997) 76.
7. J. PILITSIS, D. LUCAS and S. RENGACHARY, *Neurosurg. Focus* **13**(6) (2002) art. 1.
8. G. A. HELM, H. DAYOUB and J. A. JANE, *Neurosurg Focus* **10**(4) (2001) Article 4.
9. S. A. MASIELLO and J. A. EPSTEIN, "Letter to regeneration Technologies," Inc. 6 Pooling of Tissue form Multiple Donors During Processing Prohibited. Rockwille, MF: Food and Drug Administration (2001).
10. H. RAMAY and M. ZHANG, *Biomater*. **54** (2003) 3293.
11. P. SEPULVEDA, J. G. P. BOINNER, S. O. ROGERO, O. Z. HIGA and J. C. BRESSIANI, *J. Biomed. Mater. Res.* **50** (2000) 27.
12. S. BOSE, J. DARSELL, M. KINTNER, H. HOSICK and A. BANDYOPADHYAY, *Mat. Sci. Eng. C.* **23** 2003 479.
13. O. GAUTHIER, J. M. BOULER, E. AGUADO, P. PILET and G. DACULSI, *Biomater.* **19** (1998) 133.
14. Z. CONG, W. JIANXIN, F. HUAIZHI, L. BING and Z. XINGDONG, *J. Biomed. Mater. Res.* **55** (2001) 28.
15. M. VALLET-REGI, A. RAMILA, S. PADILLA and B. MUNOZ, *ibid.* **66** (2003) 580.
16. L. L. HENCH, *ibid.* **41** (1998) 511.
17. M. M. PEREIRA, A. E. CLARK and L. L. HENCH, *ibid.* **18** (1994) 693.
18. M. M. PEREIRA and L. L. HENCH, *J. Sol-Gel Sci. Technol.* **7** (1996) 59.
19. B. FLAUTRE, M. DESCAMPS, C. DELECOURT, M. C. BLARY and P. HARDOUIN, *J Mater Sci: Mater. Med.* **12** (2001) 679.
20. N. OZGUR ENGIN and C. TAS, *J. Eur. Cer. Soc.* **19** (1999) 2569.
21. H. YUAN, J. DE BRUIJN, X. ZHANG, C. VAN BLITTERSWIJK and K. DE GROOT, *J. Biomed. Mater. Res. (Appl. Biomater.)* **58** (2001) 270.
22. E. LANDI, G. CELOTTI, G. LOGROSCINO and A. TAMPIERI, *J. Eur. Cer. Soc.,* **23** (2003) 2931.
23. P. SEPULVEDA, J. G. P. BINNER, S. O. ROGERO, O. Z. HIGA and J. C. BRESSIANI, *J. Biomed. Mater. Res.* **50** (2000) 27.
24. J. MA, C. WANG and K. W. PENG, *Biomater.* **24** (2003) 3505.
25. N. L. PORTE, R. M. PILLIAR and M. D. GRYNPAS, *J. Biomed. Mater. Res.* **56** (2001) 504.
26. O. LYCKFELDT and J. M. L. FERREIRA, *J. Eur. Cer. Soc.* **18** (1998) 131.
27. A. F. LEMOS and J. M. F. FERREIRA, *Mat. Sci. and End C* **11** (2000) 35.
28. D. A. PRADO, M. H. SILVA, A. F. LEMOS, I. R. GIBSON, J. M. F. FERREIRA and J. D. SANTOS, *J. Non Crys. Sol.* **304** (2002) 286.
29. E. VERNÈ, C. VITALE BROVARONE and D. MILANESE, *J. Biomed. Mat. Res. (Appl. Biomater.)* **53** (2000) 408.
30. E. VERNÈ, E. BONA, A. BELLOSI, C. VITALE BROVARONE and P. APPENDINO, *J. Mat. Sci.* **36** (2001) 2801.
31. J. VORMANN, **24** (2003) 27.
32. E. JALLOT, *Appl. Sur. Sci.*, **21** (2003) 89.
33. T. KOKUBO, H. KUSHITANI and S. SAKKA, *J. Biomed. Mater. Res.* **24** (1990) 721.
34. M. BOSETTI, E. VERNÈ, M. FERRARIS, A. RAVAGLIOLI and M. CANNAS, *Biomater.* **22** (2001) 987.
35. R. L. KEPNER and J. R. PRATT, *Microbiol. Rev.* **58** (1994) 603.
36. J. L. NATION, *Stain. Technol.* **58**(6) (1983) 347.
37. W. C. A. VROUWENVELDER, C. G. GROOT and K. DE GROOT *J. Biomed. Mater. Res.* **27** (1993) 465.
38. S. FUJIABAYASHI, M. NEO, H. M. KIM, T. KOKUBO and T. NAKAMURA, *Biomater.* **24** (2003) 1349.
39. T. KOKUBO, H. M. KIM and M. KAWASHITA, *ibid.* **24** (2003) 2161.
40. O. PEITL, E. ZANOTTO and L. L. HENCH, *J. Non Crys. Sol.*, **292** (2001) 115.
41. C. ZHANG, J. WANG, H. FENG, B. LU, Z. SONG and X. ZHANG, *J. Biomed. Mater. Res.* **54** (2001) 407.
42. E. CARRIERE, J. LEMAITRE and P. H. ZYSSET, *Biomater.* **24** (2003) 809.
43. A. B. LANSDOWN, *Zinc in the Healing Wound. Lancet.* **347** (1996) 706.
44. C. R. HOWLETT, N. CHEN, X. ZHANG, F. A. AKIN, D. HAYNES, L. HANLEY, P. REVELL, P. EVANS, H. ZHOU and H. ZREIQAT, in "Bone Tissue Engineering" (Davies JE, Toronto, 2000) p. 240.
45. H. ZREIQAT, C. R. HOWLETT, A. ZANNETTINO, P. EVANS, G. SCHULZE-TANZIL, C. KNABE and M. SHAKIBAEI, *J. Biomed. Mater. Res.* **62** (2002) 175.
46. H. ZREIQAT, P. EVANS and C. R. HOWLETT, *ibid.* **44** (1999) 389.

Received 12 November 2003
and accepted 30 June 2004